Smile interpolation and calibration of the local volatility model

Nabil Kahalé

March 28, 2005

ESCP-EAP, 79 avenue de la République, 75011 Paris, France, nkahale@escp-eap.net

Abstract

The Black-and-Scholes formula provides a correspondence between the price of a plain option and the underlying asset volatility. Volatilities implied from prices of quoted plain options are, in general, not constant and depend on the strike and maturity of the option. We describe a new construction of an implied volatility surface from a discrete set of implied volatilities which is arbitrage-free and satisfies some smoothness conditions. Our algorithm allows the calibration to the smile of the local volatility model, a standard extension of the Black-and-Scholes model known to be hard to calibrate in practice. Plain options prices calculated from our local volatility surface using deterministic schemes or Monte Carlo simulation closely match input prices. This allows the pricing of exotic options in a way consistent with the price of quoted plain options.

1 Introduction

Plain or vanilla European options deliver payoffs dependent on the underlying asset price at the option maturity. The Black-and-Scholes formula determines the price of a vanilla European option by assuming the underlying volatility to be constant. It is well known, however, that implied volatilities of quoted European options are non-constant and depend both on the strike and maturity of the option, a phenomenon often referred to as the "smile". Various models based on jump-diffusion, local or stochastic volatility, have been proposed to explain and calibrate the smile (see (Andersen and Andreasen 2000, Derman and Kani 1994, Dumas, Fleming and Whaley 1998, Dupire 1994, Heston 1993, Lagnado and Osher 1997, Li 2001, Rebonato 1999, Rubinstein 1994) and references therein.) Several problems arise in the presence of smile. First, arbitrage may exist among the quoted options. Another problem is to price European options for strikes and maturities not quoted in the market. Standard interpolation techniques may give rise to arbitrage in the interpolated volatility surface even if there is no arbitrage in the original set. A related problem is to price non-vanilla options by taking the smile into account.

This paper presents a new interpolation method for implied volatilities. If the market volatilities are arbitrage-free we calculate an interpolating surface of the market volatilities for all strikes and maturities up to the last maturity that is arbitrage-free and satisfies some smoothness conditions. The basis block for

our interpolation is a single-maturity interpolation with the following properties (the first holds only if there are no absolute discrete dividends):

- If the input implied volatilities are constant so are the interpolated volatilities.
- The second derivative of the call price with respect to the strike is positive and continuous, as shown by numerical experiments.

The motivation behind the second property is that the second derivative of the call price is proportional to the implied density of the spot.

Our single-maturity interpolation does not depend on the shape of the discrete volatilities and applies to index, equity, forex and interest rate options. It takes seconds to calibrate a 10×10 volatilities matrix on a 800 Mhz processor and the quality of the fit is excellent. While our interpolation is of independent interest one of its main applications is the calibration of the local volatility model (Derman and Kani 1994, Dupire 1994, Rubinstein 1994), where the volatility of the spot is a deterministic function of the spot and time. The local volatilities can be calculated from the implied volatility surface via Dupire's formula (Dupire 1994) which is very sensitive to the interpolation used. It is well known (Avellaneda, Friedman, Holmes and Samperi 1997) that, for standard interpolation methods, Dupire's formula often leads to instabilities in the local volatilities. Our interpolated volatility surface has been designed to calibrate Dupire's model. Numerical experiments show that prices of plain options calculated via our local volatility surface and deterministic schemes or Monte Carlo simulation are very close to input prices. This allows the pricing of exotic options, including options on several assets, in a way consistent with the smile.

An alternative approach (Achdou and Pironneau 2002, Avellaneda, Friedman, Holmes and Samperi 1997, Coleman, Li and Verma 1999, Crépey 2003a, Crépey 2003b, Lagnado and Osher 1997) to calibrating Dupire's model is to calculate directly a local volatility surface that satisfies a regularity condition and produces prices close to input prices. This approach generates an arbitrage-free implied volatility surface but is more time-consuming than ours.

The rest of the paper is organised as follows. Section 2 contains preliminary results. Section 3 gives an arbitrage-free one-dimensional interpolation which has a provably continuous first derivative. Section 4 gives an arbitrage-free one-dimensional interpolation which numerical experiments show to have a continuous second derivative. Section 5 describes our two-dimensional interpolation algorithm and its application to the local volatility model. Sections 2 through 5 assume we are in the equity market and there are no interest rates and no dividends. We point out how dividends and interest rates are taken into account in Section 6. We show in Section 7 that our method can be used in the forex market and, in the one-dimensional case, in the interest rate market. An example from (Avellaneda, Friedman, Holmes and Samperi 1997) on the USD/DEM exchange rate is given in Section 8. An example on the S&P 500 has been given in a short version of our paper (Kahale 2004). Section 9 contains concluding remarks.

2 Preliminaries

We use the following definition of arbitrage, which is slightly different from the one usually found in the literature. We define an arbitrage as a self-financing portfolio of securities that has a negative value today and a nonnegative value at a given time in the future independently of the market behavior. Thus one is certain to make profit by buying such a portfolio.

It can been shown that if the input implied volatilities are given for all maturities and strikes there is no arbirage in the input if and only if the following conditions hold:

1. For a given maturity the call price is non-increasing and convex with respect to the strike.
2. The call price is a non-decreasing function of time.

The convexity condition follows from the convexity of the payoff at maturity. Based upon this result one can find in linear time whether there exists an arbitrage within a discrete set of implied volatilities. In particular the following can be shown in the one-dimensional case.

Lemma 1. *Consider a sequence $(k_i, c_i)_{0 \leq i \leq n+1}$ such that*

$$0 = c_{n+1} = k_0 < k_1 < \cdots < k_n < k_{n+1} = \infty \tag{1}$$

and c_i, $0 \leq i \leq n$, is the price of a call with strike k_i. There is no arbitrage among these prices if and only if c_0 is equal to the current spot, $c_n \geq 0$ and

$$-1 \leq \frac{c_i - c_{i-1}}{k_i - k_{i-1}} \leq \frac{c_{i+1} - c_i}{k_{i+1} - k_i} \leq 0 \text{ for } 1 \leq i < n. \tag{2}$$

3 A one-dimensional C^1 interpolation method

We give in this section a C^1 arbitrage-free interpolation method for a given maturity. Like the cubic interpolation, our method is based on the concatenation of several functions. Moreover, these functions are convex. Our construction is inspired from the Black-and-Scholes formula. We start with the following lemma:

Lemma 2. *Given $f > 0$, $\Sigma > 0$, a and b, the function*

$$c(k) = c_{f,\Sigma,a,b}(k) = fN(d_1) - kN(d_2) + ak + b, \tag{3}$$

where

$$d_1 = \frac{\log(f/k) + \Sigma^2/2}{\Sigma}$$

and $d_2 = d_1 - \Sigma$, is a convex function of k for $k > 0$.

Proof. As in the Black-and-Scholes formula, we can check that the second derivative is positive using simple differentation:

$$c'(k) = -N(d_2) + a \tag{4}$$

$$c"(k) = \frac{N'(d_2)}{k\Sigma} \tag{5}$$

□

Lemma 3. *Let g be a real function defined for all real numbers such that $g'(x)$ exists and is positive for any real number x and $1/g'$ is strictly convex. For $\lambda \in]0,1[$ and any real numbers $x_0 < x_1$, the function $h(a) = g(\lambda g^{-1}(a+x_0) + (1-\lambda)g^{-1}(a+x_1)) - a$ has a positive derivative with respect to a on the (possibly empty) interval on which it is defined.*

Proof. Let $y = g^{-1}(a+x_0)$ and $z = g^{-1}(a+x_1)$. By standard calculus

$$h'(a) = g'(\lambda y + (1-\lambda)z)(\frac{\lambda}{g'(y)} + \frac{1-\lambda}{g'(z)}) - 1.$$

The equation $h'(a) > 0$ is equivalent to

$$\frac{\lambda}{g'(y)} + \frac{1-\lambda}{g'(z)} > \frac{1}{g'(\lambda y + (1-\lambda)z)},$$

which follows from the strict convexity of $1/g'$. □

Theorem 1. *For all real numbers k_0, k_1, c_0, c_1, c'_0, and c'_1 such that $0 < k_0 < k_1$ and*

$$c'_0 < \frac{c_1 - c_0}{k_1 - k_0} < c'_1 < 1 + c'_0 \tag{6}$$

there exists a unique vector (f, Σ, a, b) with $f > 0$, $\Sigma > 0$ such that the function $c = c_{f,\Sigma,a,b}$ satisfies the following conditions: $c(k_0) = c_0$, $c(k_1) = c_1$, $c'(k_0) = c'_0$ and $c'(k_1) = c'_1$. The vector (f, Σ, a, b) is continuous with respect to $(k_0, k_1, c_0, c_1, c'_0, c'_1)$ and can be calculated numerically.

Proof. Given $a \in]c'_1, 1 + c'_0[$, let d_2^0, d_2^1, α and β be the unique reals numbers such that

$$c'_i = -N(d_2^i) + a \tag{7}$$

and

$$d_2^i = \alpha \log(k_i) + \beta,$$

for $i \in \{0, 1\}$. The existence of d_2^i is a consequence of the inequalities $c'_i < a < c'_i + 1$ which follow from Eq. 6. Since $c'_0 < c'_1$ we have $d_2^0 > d_2^1$ by Eq. 7, and thus

$$\alpha = \frac{d_2^0 - d_2^1}{\log(k_0) - \log(k_1)} < 0. \tag{8}$$

Hence there exist $f > 0$ and $\Sigma > 0$ such that $\alpha = -1/\Sigma$ and $\beta = (\log f)/\Sigma - \Sigma/2$. It follows that

$$d_2^i = \frac{\log(f/k_i) - \Sigma^2/2}{\Sigma}. \tag{9}$$

Note that d_2^i, α, β, f and Σ are continuous functions of a as a ranges in $]c'_1, 1+c'_0[$. Consider the function $c = c_{f,\Sigma,a,b}$, where b is chosen so that $c(k_0) = c_0$. It follows from Eqs. 9 and 4 that $c'(k_i) = -N(d_2^i) + a$, and so $c'(k_i) = c'_i$ by Eq. 7. We now show that, for some $a \in]c'_1, 1+c'_0[$, $c(k_1) = c_1$. The ratio $(c(k_1) - c(k_0))/(k_1 - k_0)$ is a continuous function of a. It follows from Eq. 4 that, for $k_0 < k < k_1$,

$$c'(k) = a - N(\lambda N^{-1}(a - c'_0) + (1-\lambda)N^{-1}(a - c'_1)),$$

where $\lambda = \log(k_1/k)/\log(k_1/k_0)$. By applying Lemma 3 to the Normal function, we infer that $c'(k)$ is a strictly decreasing and has a negative derivative with

respect to a. The same holds for the ratio $(c(k_1) - c(k_0))/(k_1 - k_0)$. When $a \to c_1'$, $c'(k) \to c_1'$ for $k \neq k_0$. It follows that

$$\frac{c(k_1) - c(k_0)}{k_1 - k_0} \to c_1' \text{ as } a \to c_1'.$$

Similarly,

$$\frac{c(k_1) - c(k_0)}{k_1 - k_0} \to c_0' \text{ as } a \to 1 + c_0'.$$

By continuity and Eq. 6, there exists $a_0 \in]c_1', 1 + c_0'[$ such that, for $a = a_0$,

$$\frac{c(k_1) - c(k_0)}{k_1 - k_0} = \frac{c_1 - c_0}{k_1 - k_0}.$$

Since $c(k_0) = c_0$, the equality $c(k_1) = c_1$ holds for $a = a_0$. Standard algorithms for inverting functions (Press, Flannery, Teukolsky and Vetterling 1993) can be used to calculate a_0 numerically. The uniqueness and continuity of a_0 with respect to $(k_0, k_1, c_0, c_1, c_0', c_1')$ follows from the fact that the derivative of the ratio $(c(k_1) - c(k_0))/(k_1 - k_0)$ is negative with respect to a. □

Theorem 1 gives an interpolation method between two strikes. We extend it below to extrapolate the call prices below or beyond a certain strike. The extrapolation method satisfies limit conditions that also hold in the constant-volatility case.

Lemma 4. *For all real numbers k_0, c_0, and c_0' such that $0 < k_0$, $-1 < c_0' < 0$ and $c_0 > 0$ there exist two unique parameters $f > 0$ and $\Sigma > 0$ such that the function $c = c_{f,\Sigma,0,0}$ satisfies the following conditions: $c(k_0) = c_0$, $c'(k_0) = c_0'$. Moreover $c(k) \to 0$ and $c'(k) \to 0$ as $k \to \infty$. The vector (f, Σ) is continuous with respect to (k_0, c_0, c_0') and can be calculated numerically.*

Proof. Let d_2^0 be the unique real number such that $c_0' = -N(d_2^0)$. For $\Sigma > 0$, let $f = k_0 \exp(\Sigma d_2^0 + \Sigma^2/2)$. The function $c = c_{f,\Sigma,0,0}$ has a derivative equal to c_0' at k_0. As $\Sigma \to 0$, $c(k_0) \to 0$ and, as $\Sigma \to \infty$, $c(k_0) \to \infty$. Thus $c(k_0) = c_0$ when $\Sigma = \Sigma_0$, for some $\Sigma_0 > 0$. In order to show the uniqueness of Σ_0 we prove that $c(k_0)$ has a positive derivative with respect to Σ. Let $d_1 = d_2^0 + \Sigma$, so that $c(k_0) = fN(d_1) + k_0 c_0'$. The logarithmic derivative of $fN(d_1)$ with respect to Σ is $N'(d_1)/N(d_1) + d_1$, which is positive by standard calculus. The uniqueness and continuity of Σ_0 with respect to (k_0, c_0, c_0') follows. The calculation of the limits of $c(k)$ and $c'(k)$ as $k \to \infty$ follows by standard arguments. □

Lemma 5. *For all real numbers k_1, c_0, c_1 and c_1' such that $0 < k_1$ and*

$$-1 < \frac{c_1 - c_0}{k_1} < c_1' < 0, \tag{10}$$

there exist three unique parameters $f > 0$, $\Sigma > 0$ and b such that the function $c = c_{f,\Sigma,0,b}$ satisfies the following conditions: $c(k) \to c_0$ as $k \to 0$, $c'(k_1) = c_1'$, $c(k_1) = c_1$. Moreover, $c'(k) \to -1$ as $k \to 0$. the vector (f, Σ, b) is continuous with respect to (k_1, c_0, c_1, c_1') and can be calculated numerically.

Proof. Let d_2^1 be the unique real number such that $c_1' = -N(d_2^1)$. For $\Sigma > 0$ let

$$f = k_1 \exp(\Sigma d_2^1 + \Sigma^2/2) \tag{11}$$

and

$$b = c_0 - f. \tag{12}$$

The function $c = c_{f,\Sigma,0,b}$ has a derivative equal to c_1' at k_1. Moreover, $(c(k), c'(k)) \to (c_0, -1)$ as $k \to 0$ by standard calculations. It remains to show that $c(k_1) = c_1$ for some $\Sigma > 0$. Since $c(k_1) = fN(d_1) + k_1 c_1' + b$, with $d_1 = d_2^1 + \Sigma$,

$$c(k_1) - c_0 = -fN(-d_2^1 - \Sigma) + k_1 c_1' \tag{13}$$

by Eq. 12. Eq. 11 determines f as a function of Σ. As $\Sigma \to 0$, $f \to k_1$ and

$$c(k_1) - c_0 \to -k_1 N(-d_2^1) + k_1 c_1' = -k_1.$$

Since $N(x) \sim N'(x)/|x|$ as $x \to -\infty$,

$$c(k_1) - c_0 \to k_1 c_1' \text{ as } \Sigma \to \infty.$$

By continuity and Eq. 10 it follows that $c(k_1) = c_1$ when $\Sigma = \Sigma_0$, for some $\Sigma_0 > 0$. As in Lemma 4, it can be show that the derivative of $c(k_1)$ with respect to Σ is positive. This implies the uniqueness and continuity of Σ_0 with respect to (k_1, c_0, c_1, c_1'). □

Combining Lemmas 2, 4, 5 and Theorem 1, we obtain the following definition and theorem.

Definition 1. *For all real numbers k_0, k_1, c_0, c_1, c_0', and c_1' such that $0 < k_0 < k_1$ and Eq. 6 holds, denote by $\phi(k_0, c_0, c_0', k_1, c_1, c_1')$ the function $c = c_{f,\Sigma,a,b}$ that satisfies the following conditions: $c(k_0) = c_0$, $c(k_1) = c_1$, $c'(k_0) = c_0'$ and $c'(k_1) = c_1'$. Similarly, for all real numbers k_0, c_0, and c_0' such that $0 < k_0$, $-1 < c_0' < 0$ and $c_0 > 0$, denote by $\phi(k_0, c_0, c_0', \infty, 0, 0)$ the function $c = c_{f,\Sigma,0,0}$ that satisfies the following conditions: $c(k_0) = c_0$, $c'(k_0) = c_0'$. Finally, for all real numbers k_1, c_0, c_1 and c_1' such that $0 < k_1$ and Eq. 10 holds, denote by $\phi(0, c_0, -1, k_1, c_1, c_1')$ the function $c = c_{f,\Sigma,0,b}$ that satisfies the following conditions: $c(k) \to c_0$ as $k \to 0$, $c'(k_1) = c_1'$, $c(k_1) = c_1$.*

It follows from Definition 1 that for all real or infinite numbers k_0, k_1, c_0, c_1, c_0', and c_1' such that the function $c = \phi(k_0, c_0, c_0', k_1, c_1, c_1')$ is defined, $(c(k), c'(k)) \to (c_i, c_i')$ as $k \to k_i$, $i \in \{0, 1\}$. By combining the interpolated and extrapolated methods for a series of strikes, we obtain the following.

Theorem 2. *For all sequences $(k_i)_{0 \le i \le n+1}$, $(c_i)_{0 \le i \le n+1}$ and $(c_i')_{0 \le i \le n+1}$ such that Eq. 1 holds together with the limit conditions*

$$c_0' = -1, \ c_n' < c_{n+1}' = 0 < c_n, \tag{14}$$

and the convexity conditions

$$c_i' < \frac{c_{i+1} - c_i}{k_{i+1} - k_i} < c_{i+1}' \text{ for } 0 \le i < n, \tag{15}$$

there exist a C^1 convex function $c(k)$, $k > 0$, and a unique sequence $(f_i, \Sigma_i, a_i, b_i)_{0 \le i \le n}$ such that $c(k) = c_{f_i,\Sigma_i,a_i,b_i}(k)$ on the interval $[k_i, k_{i+1}] - \{0, \infty\}$, $c(k_i) = c_i$ and $c'(k_i) = c'_i$ for $1 \le i \le n$. Moreover,

$$(c(k), c'(k)) \to (c_0, -1) \text{ as } k \to 0 \tag{16}$$

and

$$(c(k), c'(k)) \to (0, 0) \text{ as } k \to \infty. \tag{17}$$

The sequence $(f_i, \Sigma_i, a_i, b_i)_{0 \le i \le n}$ is continuous with respect to $(c_0, (k_i, c_i, c'_i)_{1 \le i \le n})$ and can be calculated numerically.

There are $4(n+1)$ unknown parameters $(f_i, \Sigma_i, a_i, b_i)_{0 \le i \le n}$ that define the function c. Each equation $c(k_i) = c_i$, $1 \le i \le n$, accounts for two conditions on these parameters, because it holds both for $c_{f_i,\Sigma_i,a_i,b_i}(k_i)$ and $c_{f_{i-1},\Sigma_{i-1},a_{i-1},b_{i-1}}(k_i)$. The same holds for the equation $c'(k_i) = c'_i$, $1 \le i \le n$. Together with the limit conditions as $k \to 0$ and as $k \to \infty$, there are $4n + 4$ conditions, which is equal to the number of parameters.

4 A one-dimensional C^2 interpolation method

The algorithm in Theorem 2 gives a C^1 convex interpolating curve at a given maturity. But, since the second derivative of the call price with respect to the strike is proportional to the density of the strike in the risk-neutral word, a C^2 interpolating curve is desired. We give in this section an interpolating algorithm for the call prices at a given maturity which we conjecture will converge towards a C^2 interpolating curve with the properties mentioned in Section 1. We start with a few lemmas to motivate our algorithm.

Lemma 6. *Let g be a convex C^1 function defined on the interval $[x_0, x_1]$, and $x_2 \in]x_0, x_1[$. The following holds:*

$$g'(x_1) - g'(x_2) \le \eta \left(g'(x_1) - \frac{g(x_1) - g(x_0)}{x_1 - x_0} \right), \tag{18}$$

where $\eta = (x_1 - x_0)/(x_2 - x_0)$.

Proof. Since $g(x_2) - g(x_0) \le g'(x_2)(x_2 - x_0)$ and $g(x_1) - g(x_2) \le g'(x_1)(x_1 - x_2)$,

$$g(x_1) - g(x_0) \le g'(x_2)(x_2 - x_0) + g'(x_1)(x_1 - x_2),$$

and so

$$g(x_1) - g(x_0) - g'(x_1)(x_1 - x_0) \le (g'(x_2) - g'(x_1))(x_2 - x_0)$$

which is equivalent to Eq. 18. □

Lemma 7. *For any $\gamma > 0$ there exists $\epsilon_0 > 0$ such that, for $\epsilon < \epsilon_0$, $\delta > 0$ and all u, if*

$$N(u + \delta) - N(u) < \epsilon \text{ and} \tag{19}$$

$$N(u + 2\delta) - N(u) > \gamma \tag{20}$$

then $\delta N'(u) < \epsilon$.

Proof. Assume without loss of generality that $\epsilon_0 < \gamma/2 < 1$. By Eq. 20, $N(u + 2\delta) - N(u + \delta) > \gamma/2$ and so

$$u + \delta < z_0, \tag{21}$$

where $z_0 = N^{-1}(1 - \gamma/2)$. Let $z \in [u, u + \delta]$ be such that $N(u + \delta) - N(u) = \delta N'(z)$. By Eq. 19,

$$\delta N'(z) < \epsilon. \tag{22}$$

Since the function N' is upper bounded by 1, it follows from Eq. 20 that $\delta > \gamma/2$, and so $N'(z) < 2\epsilon/\gamma$. But $z < z_0$ by Eq. 21. Let $\epsilon_0 = \gamma N'(z_0)/2$. If $\epsilon < \epsilon_0$ then $N'(z) < N'(z_0)$ and so $z < 0$. Hence $N'(u) \leq N'(z)$. By Eqs. 22 it follows that $\delta N'(u) < \epsilon$. □

Lemma 8. *Given any real numbers k_0, k_1, c_0, c_1, c'_0 such that $0 < k_0 < k_1$ and*

$$c'_0 < \frac{c_1 - c_0}{k_1 - k_0} < 1 + c'_0, \tag{23}$$

let $c'_1 \in](c_1 - c_0)/(k_1 - k_0), 1 + c'_0[$ and $c = \phi(k_0, c_0, c'_0, k_1, c_1, c'_1)$. Then $c"(k_1) \to 0$ as $c'_1 \to (c_1 - c_0)/(k_1 - k_0)$.

Proof. We show there exists $\epsilon_0, \theta > 0$ such that, for $0 < \epsilon < \epsilon_0$ if

$$\frac{c_1 - c_0}{k_1 - k_0} < c'_1 < \frac{c_1 - c_0}{k_1 - k_0} + \epsilon$$

then $c"(k_1) < \theta\epsilon$. By choosing $\epsilon_0 < 1 + c'_0 - (c_1 - c_0)/(k_1 - k_0)$, the existence of $c = c_{f,\Sigma,a,b}$ follows from Theorem 1. Let $\gamma = (c_1 - c_0)/(k_1 - k_0) - c'_0$. By convexity $c'(k_1) - c'(k_0) > \gamma$. Using the same notation as in Theorem 1 and Eq. 4, it follows that

$$N(d_2^0) - N(d_2^1) > \gamma.$$

Let $k_2 = \sqrt{k_0 k_1}$. By Lemma 6, $c'(k_1) - c'(k_2) < \eta\epsilon$, where $\eta = (k_1 - k_0)/(k_2 - k_0)$, and so

$$N(\frac{d_2^0 + d_2^1}{2}) - N(d_2^1) < \eta\epsilon.$$

By Lemma 7, it follows that $(d_2^0 - d_2^1)N'(d_2^1) < 2\eta\epsilon$ for a suitable ϵ_0. Using Eq. 5, it follows after some calculations that $c"(k_1) < \theta\epsilon$, where $\theta = 2\eta/(k_1 \log(k_1/k_0))$. □

Lemma 8 shows that $c"(k_1) \to 0$ as $c'(k_1)$ goes to its lower limit. Lemma 9 below shows a similar result holds in the limit case when $k_0 = 0$.

Lemma 9. *For all real numbers k_1, c_0 and c_1 such that $0 < k_1$ and*

$$-1 < \frac{c_1 - c_0}{k_1} < 0,$$

let c'_1 range in $](c_1 - c_0)/k_1, 0[$ and c the function $\phi(0, c_0, -1, k_1, c_1, c'_1)$. Then $c"(k_1) \to 0$ as $c'_1 \to (c_1 - c_0)/k_1$.

Proof. We use the same notation as in Lemma 5, from which follows the existence of c. Eq. 13 implies that, as $c'_0 \to (c_1 - c_0)/k_1$, $fN(-d_2^1 - \Sigma) \to 0$. Since, by Eq. 11 f is lower-bounded by $k_1 \exp(-(d_2^1)^2/2)$, it follows that $\Sigma \to \infty$. Thus $c"(k_0) \to 0$ by Eq. 5. □

Lemma 10. *Given any real numbers k_0, k_1, c_0, c_1, c'_1 such that $0 < k_0 < k_1$ and*

$$c'_1 - 1 < \frac{c_1 - c_0}{k_1 - k_0} < c'_1 \tag{24}$$

let $c'_0 \in]c'_1 - 1, (c_1 - c_0)/(k_1 - k_0)[$ and $c = \phi(k_0, c_0, c'_0, k_1, c_1, c'_1)$. Then $c"(k_0) \to 0$ as $c'_0 \to (c_1 - c_0)/(k_1 - k_0)$.

Proof. The proof is similar to the proof of Lemma 8 and is omitted. □

Lemma 10 shows that $c"(k_0) \to 0$ as $c'(k_0)$ goes to its upper limit. Lemma 11 below shows a similar result holds in the limit case when $k_1 = \infty$.

Lemma 11. *For all real numbers k_0, c_0 such that $0 < k_0$ and $c_0 > 0$, let c'_0 range in $]-1, 0[$ and $c = c_{f,\Sigma,0,0}$ be the function $\phi(k_0, c_0, c'_0, \infty, 0, 0)$. Then $c"(k_0) \to 0$ as $c'_0 \to 0$.*

Proof. Using the same notation as in Lemma 4, standard algebra shows that, as $c'_0 \to 0$, $d_2^0 \to -\infty$, $fN(d_1) \to c_0$, $\Sigma \to \infty$, and thus $c"(k_0) \to 0$ by Eq. 5. □

Theorem 3 below shows how to construct a concatenated function that will be twice continuous at a given point k_j, for some j in the interval $[1, n]$. Step 2 of algorithm A described in Subsection 4.1 guarantees the concatenated function to be twice continuous at all points k_j, for any j in the interval $[1, n]$.

Theorem 3. *Let j be an integer in the interval $[1, n]$. For all sequences $(k_i)_{0 \le i \le n+1}$, $(c_i)_{0 \le i \le n+1}$ and $(c'_i)_{0 \le i \le n+1}$ such that Eqs. 1, 14 and 15 hold, there exist a C^1 convex function $c(k)$, $k > 0$, and a sequence $(f_i, \Sigma_i, a_i, b_i)_{0 \le i \le n}$ such that $c(k) = c_{f_i,\Sigma_i,a_i,b_i}(k)$ on the interval $[k_i, k_{i+1}] - \{0, \infty\}$, $c(k_i) = c_i$ for $1 \le i \le n$, $c'(k_i) = c'_i$ for $1 \le i \le n$, $i \ne j$, and c has a continuous second derivative at k_j. Moreover, the limit properties in Eqs. 16 and 17 hold. The sequence $(f_i, \Sigma_i, a_i, b_i)_{0 \le i \le n}$ can be calculated numerically.*

Proof. For $1 \le i \le n$, let $l_i = (c_i - c_{i-1})/(k_i - k_{i-1})$. By Theorem 2, for any $\gamma \in]l_j, l_{j+1}[$, there exist a C^1 convex function $c(k)$, $k > 0$, and a sequence $(f_i, \Sigma_i, a_i, b_i)_{0 \le i \le n}$ such that $c(k) = c_{f_i,\Sigma_i,a_i,b_i}(k)$ on the interval $[k_i, k_{i+1}] - \{0, \infty\}$, $c(k_i) = c_i$ for $1 \le i \le n$, $c'(k_j) = \gamma$ and $c'(k_i) = c'_i$ for $1 \le i \le n$, $i \ne j$, and the limit conditions defined in Eqs. 16 and 17 hold. We show that for some $\gamma \in]l_j, l_{j+1}[$, c has a continuous second derivative at k_j.

As γ goes to l_j, the left second derivative $c"({k_j}^-)$ of c at k_j goes to 0 by Lemmas 8 and 9. But the right second derivative $c"({k_j}^+)$ of c at k_j goes to $\psi"(k_j)$, where ψ is the function $\phi(k_j, c_j, l_j, k_{j+1}, c_{j+1}, c'_{j+1})$. Hence, $c"({k_j}^+) - c"({k_j}^-)$ has a positive limit as γ goes to l_j. Similarly, it can be shown that $c"({k_j}^+) - c"({k_j}^-)$ has a negative limit as γ goes to l_{j+1}. By continuity, $c"({k_j}^+) = c"({k_j}^-)$ for some value of $\gamma \in]l_j, l_{j+1}[$. □

As in Theorem 2, the number of constraints on the parameters in Theorem 3 is equal to the number of parameters because there are still four constraints at k_j: $c({k_j}^+) = c({k_j}^-) = c_j$, $c'({k_j}^+) = c'({k_j}^-)$ and $c"({k_j}^+) = c"({k_j}^-)$. Unlike Theorem 2, though, it is not clear whether the function constructed in Theorem 3 is unique.

4.1 The algorithm description

We are now ready to describe our algorithm. Consider sequences $(k_i)_{0\le i\le n+1}$ and $(c_i)_{0\le i\le n+1}$ such that Eq. 1 holds, $c_n > 0$ and

$$-1 < \frac{c_i - c_{i-1}}{k_i - k_{i-1}} < \frac{c_{i+1} - c_i}{k_{i+1} - k_i} < 0 \text{ for } 1 \le i < n. \tag{25}$$

Note that Eq. 25 is the same as Eq. 2 except that inequalities have been replaced by strict inequalities. Let $\epsilon > 0$ be an error parameter. Algorithm A consists of the following procedures:

1. Initialization Step. Let $c'_0 = -1$, $c'_{n+1} = \infty$ and $c'_i = (l_i + l_{i+1})/2$, for $1 \le i \le n$, where $l_i = (c_i - c_{i-1})/(k_i - k_{i-1})$.

2. Loop. For $1 \le j \le n$, let $\gamma_j = c'_j(k_j)$, where c_j is a function calculated in Theorem 3 for the index j. Replace simultaneously (c'_j) by γ_j, $1 \le j \le n$. Repeat this step until $\max_{1\le j\le n}(|c"({k_j}^+) - c"({k_j}^-|) < \epsilon$.

Conjecture 1. *For all sequences $(k_i)_{0\le i\le n+1}$, $(c_i)_{0\le i\le n+1}$ such that Eqs. 1 and 25 hold, the sequences calculated by Algorithm A converge in the limit towards a sequence $(f_i, \Sigma_i, a_i, b_i)_{0\le i\le n}$. There exists a C^2 convex function $c(k)$, $k > 0$, such that $c(k) = c_{f_i,\Sigma_i,a_i,b_i}(k)$ on the interval $[k_i, k_{i+1}] - \{0, \infty\}$ and $c(k_i) = c_i$ for $1 \le i \le n$. Moreover, the limit properties in Eqs. 16 and 17 hold.*

The number of constraints on the parameters in conjecture 1 is equal to the number of parameters. To see this, we note there are still four constraints at k_j, $1 \le j \le n$: $c({k_j}^+) = c({k_j}^-) = c_j$, $c'({k_j}^+) = c'({k_j}^-)$ and $c"({k_j}^+) = c"({k_j}^-)$. Since there are four limit constraints by Eq. 17, the total number of constraints is equal to $4n + 4$, which is equal to the number of parameters. It is not clear, though, whether there exists a unique function c satisfying the properties in conjecture 1. Several methods can be used to improve the numerical stability and speed of convergence of Algorithm A. We have tested a variant of Algorithm A where the c'_j and γ_j are updated in parallel using a Newton-Raphson method. Our experiments support our conjecture.

5 A two-dimensional interpolation method and Dupire's model

If no arbitrage is found in the input implied volatilities we calculate an arbitrage-free interpolating volatility surface using Algorithm B that consists of the following steps:

1. We generate a one-dimensional arbitrage-free interpolation for each input maturity t_i using the above variant of Algorithm A.

2. For each maturity $t \in]t_i, t_{i+1}[$ and each strike K, we calculate the implied volatility $\sigma_{\text{imp}}(K, T)$ so that $\sigma^2_{\text{imp}}(K, T)T$ is a linear interpolation of $\sigma^2_{\text{imp}}(K, t_i)t_i$ and $\sigma^2_{\text{imp}}(K, t_{i+1})t_{i+1}$.

3. We make the necessary adjustments so that the entire volatility surface is arbitrage-free.

Our interpolation in the time domain ensures that if the no-arbitrage condition $C(K,t_i) < C(K,t_{i+1})$ holds, where $C(K,T)$ is today' s price of a European call with strike K and maturity T, $C(K,T)$ is an increasing function of T between t_i and t_{i+1}. This is because, in the Black-and-Scholes formula, $C(K,T)$ depends on time only through $\sigma^2_{\text{imp}}(K,T)T$. Moreover, $C(K,T)$ is an increasing function of $\sigma^2_{\text{imp}}(K,T)T$. Thus the no-arbitrage condition with respect to time holds if and only if $\sigma^2_{\text{imp}}(K,T)T$ is an increasing function of T. Step 3 is shown in detail in Subsection 5.1.

Because of the adjustments made in the last step, the smoothness properties of the one-dimensional interpolation method described in Section 1 may not hold for the two-dimensional interpolation method. However, numerical experiments in the two-dimensional case show that, for any maturity up to the last input maturity, the second derivative of the call price with respect to the strike exists and is continuous and positive except for a few points. Moreover, the derivative with respect to time is continuous except at input maturities. These properties help to ensure the stability of pricing exotic options using Dupire's model. In Dupire's model (Dupire 1994) the spot follows the following stochastic differential equation:

$$dS_t = \mu_t S_t dt + \sigma(S_t,t) S_t dW_t,$$

where W_t is a Brownian motion and $\sigma(S,t)$ is a deterministic function. Dupire has shown that if the implied volatilities are known for all strikes and maturities then the local volatility surface is uniquely determined. More precisely,

$$\sigma^2(K,T) = 2\frac{\frac{\partial C(K,T)}{\partial T}}{K^2 \frac{\partial^2 C(K,T)}{\partial K^2}}.$$

Several pros and cons of Dupire's model can be found in the literature. A classical problem in implementing the model is the instability of the local volatilities calculation. According to the practical cases we tested our interpolating algorithm is well suited to calibrating Dupire's model. This is because the second derivative with respect to the strike of the call prices generated by our algorithm exists in practice and is continuous and positive for maturities up to the last input maturity. Moreover the call prices derivative with respect to the maturity exists and is continuous and positive except at input maturities. The local volatility surface is therefore, in general, continuous except at input maturities, and can be calculated approximately using finite difference approximations of derivatives.

It is known that the price of a contingent claim on S obeys the following PDE:

$$\frac{\partial u(S,t)}{\partial t} + \frac{1}{2}\sigma^2(S,t)S^2\frac{\partial^2 u(S,t)}{\partial S^2} = 0,$$

where $u(S,t)$ is the price at time t of a contingent claim if the spot price is S at time t. The local volatility surface can thus be used to calculate option prices using finite difference schemes such as the Crank-Nicholson's algorithm.

5.1 Making the entire volatility surface arbitrage-free

Once the implied volatility surface has been calculated in Step 2 for all maturities up to the last input maturity t_h, we calculate the associated call prices $C(K,T)$

for $T \leq t_h$. Then, for each maturity $T \leq t_h$, we replace $C(K,T)$ by $C^*(K,T)$, where $C^*(K,T)$ is the supremum of all convex functions $\hat{C}(K,T)$ with respect to K such that $\hat{C}(K,T) \leq C(K,s)$ for $T \leq s \leq t_h$. The function $C^*(K,T)$ is convex with respect to K since the supremum of convex functions is convex. It is not hard to show that $C^*(K,T)$ is increasing with respect to T. Hence the call surface $C^*(K,T)$ is arbitrage-free for all K and $T \leq t_h$.

In our implementation we have inverted steps 2 and 3 of Algorithm B and used a variant of step 3 that guarantees the restriction of the volatility surface to the union of input maturities to be arbitrage-free. Experiments we performed on market volatilities show that the entire volatility surface generated by this variant of Algorithm B is, for practical purposes, arbitrage-free.

5.2 Deep in the money and out of the money volatilities

For a given maturity, the extrapolation methods in Sections 3 and 4 yield asymptotically constant implied volatilities as the strike goes to infinity. This follows from standard calculus and the asymptotics

$$c_{f,\Sigma,0,0}(k) \sim fN'(d_1)\frac{\Sigma}{d_1 d_2}, \tag{26}$$

as $k \to \infty$. Eq. 26 can be shown using the expansion

$$N(z) \sim \frac{N'(z)}{|z|}(1 - \frac{1}{z^2} + O(\frac{1}{z^4}))$$

as $z \to -\infty$. A similar result holds when the strike goes to 0. In practice, for a given maturity, we determine a strike which is deep out of the money and a strike deep in the money and keep the implied volatilities constant outside these strikes. The calculated local volatilities are also constant deep in and deep out of the money for a given maturity.

6 Dealing with dividends and interest rates

We assume that interest rates are deterministic and that dividends are of one or a combination of the following types:

- Absolute dividend with a predetermined cash amount at a predetermined date.
- Proportional dividend at a predetermined date with an amount proportional to the spot.
- Continuous dividend with a predetermined dividend rate.

We further assume that absolute dividends exist up to a certain maturity, with no restrictions on proportional or continuous dividends. We reduce the computation of the local volatility surface to the case where interest rates and dividends are null using a transformation similar to the one in (Overhaus, Ferraris, Knudsen, Milward, Nguyen-Ngoc and Schindlmayr 2002, Section 4.6). Let T^* be a maturity larger than all absolute dividends and input options maturities and let S_t^* be the forward of S_t at maturity T^*. Thus S_t^* is continuous and driftless

and can be considered as an underlying in an interest rate and dividend-free world. By a classical calculation (see e.g. (Overhaus, Ferraris, Knudsen, Milward, Nguyen-Ngoc and Schindlmayr 2002, Section 4.6)) $S_t = a(t)S_t^* + b(t)$, where $a(t)$ and $b(t)$ are deterministic functions of time. Let $C^*(K^*, T)$ be the expected value under the risk neutral distribution of $\max(0, S^*(t) - K^*)$. Thus $C(K, T) = B(t_0, t)a(t)C^*(K^*, T)$, where $K = a(t)K^* + b(t)$ and $B(t_0, t)$ is the price at initial time t_0 of a zero-coupon maturing at t. A discrete set of option prices on S determines a discrete set of option prices on S^*. Using results in previous sections, we can calculate a local volatility surface $\sigma^*(S^*, t)$ that matches the options prices on S^*. By Ito's lemma, the local volatility surface $\sigma(S, t) = a(t)S^*\sigma^*(S^*, t)/S$ matches the options prices on S. It can be shown that the local volatility surface $\sigma(S, t)$ remains unchanged if T^* is replaced by a larger maturity.

In general, by non-arbitrage, volatility can no longer be a continuous function of time at dividend dates. For the same reason volatility cannot be constant everywhere in the presence of absolute dividends. Our algorithm generates an arbitrage-free implied volatility surface that has the same smoothness properties mentioned in the preceding sections except at discrete dividend dates. In practice the error rate of the calculated prices is generally higher if there are discrete dividends.

7 The foreign exchange and interest rate markets

Our algorithm can readily be used in the foreign exchange derivatives market because the foreign exchange dynamics are similar to the equity dynamics. The continuous dividend rate is simply replaced by the foreign exchange rate.

Our one-dimensional algorithm can be used to interpolate volatilities on options expiring at a given maturity T on a swap or interest rate spanning a given period I. A slight modification is needed however if we assume interest rates can be negative.

8 Example

We tested our algorithm on the market implied volatilities of the USD/DEM exchange rate on August 23, 1995 given in (Avellaneda, Friedman, Holmes and Samperi 1997) and shown in Fig. 1. The DEM deposit rate is 4.27% while the US deposit rate is 5.91%.

We plot in Fig. 2 the interpolated volatility surface, in Fig. 3 the call price, in Fig. 4 the risk-neutral density function of the spot, and in Fig. 5 the local volatility surface.

We compared the Black-and-Scholes prices calculated via the input implied volatilities to those calculated via the interpolated implied volatilities. The maximum relative error (price differences divided by the initial spot) obtained is of order 10^{-7}. We also compared the prices calculated via the input implied volatilities to the prices obtained via the Crank-Nicholson method and our local volatility surface with 50 time-steps and 500 space-steps. The maximum relative error obtained is of order 10^{-5}. Finally, we compare in Fig. 6 the prices

Maturity	Type	Strike	Implied volatility
30 days	Call	1.5421	14.9
	Call	1.5310	14.8
	Call	1.4872	14.0
	Put	1.4479	14.2
	Put	1.4371	14.4
60 days	Call	1.5621	14.4
	Call	1.5469	14.5
	Call	1.4866	13.8
	Put	1.4312	14.0
	Put	1.4178	14.2
90 days	Call	1.5764	14.1
	Call	1.5580	14.1
	Call	1.4856	13.5
	Put	1.4197	13.6
	Put	1.4038	13.6
180 days	Call	1.6025	13.1
	Call	1.5779	13.1
	Call	1.4823	13.1
	Put	1.3902	13.7
	Put	1.3682	13.7
270 days	Call	1.6297	13.3
	Call	1.5988	13.2
	Call	1.4793	13.0
	Put	1.3710	13.2
	Put	1.3455	13.2

Figure 1: Implied volatilities for the USD/DEM exchange rate on August 23, 1995.

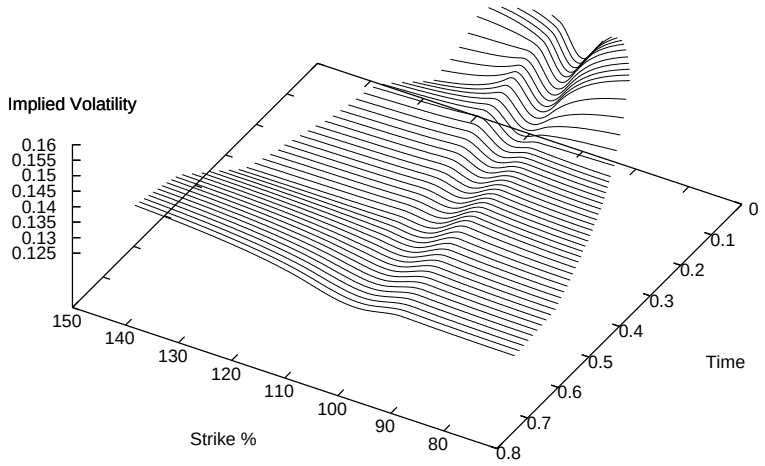

Figure 2: Interpolated implied volatilities on the USD/DEM exchange rate on August 1995 in terms of the maturity and the strike.

calculated via the input implied volatilities to those obtained via Monte Carlo simulation together with our local volatility surface. We used 50 time-steps and 100000 paths in the Monte Carlo simulation. The maximum relative error obtained is of order 10^{-4}. Our Monte Carlo simulation algorithm can be generalised to several dimensions, thereby allowing the pricing of options on several assets in a way consistent with the smile.

9 Conclusion

We have designed a one-dimensional interpolation algorithm for implied volatilities that is robust and has good smoothness properties. Our algorithm applies to equity, forex and interest rate options. It can be extended to the two-dimensional case for equity and forex options. In practice the regularity properties of our interpolation scheme ensure it can be used to calibrate Dupire's model. Vanilla options prices calculated from our local volatility surface using PDE schemes or Monte Carlo simulation closely match input prices. Our method can be used to price options on one or several assets in a way consistent with the smile.

References

Dupire, B. 1994. Pricing with a smile, *Risk* **7**(7): 18–20.

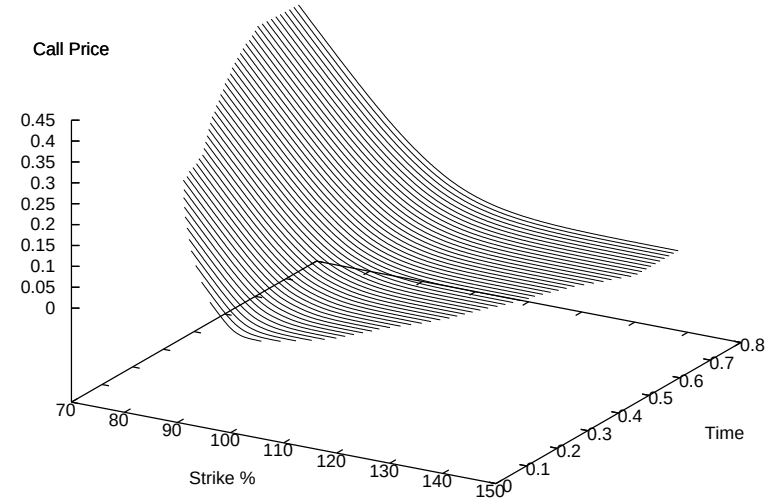

Figure 3: Call price on the USD/DEM exchange rate on August 1995 in terms of the maturity and the strike.

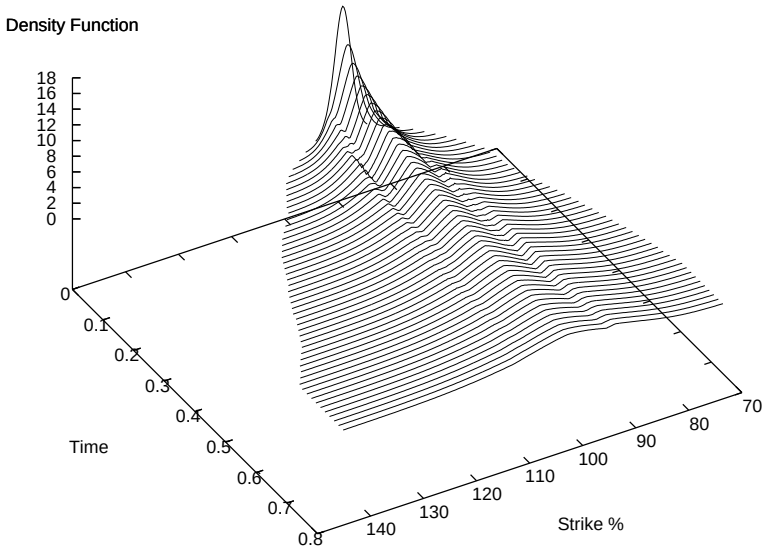

Figure 4: Implied risk-neutral density function of the spot of the USD/DEM exchange rate on August 1995 in terms of the maturity and the strike.

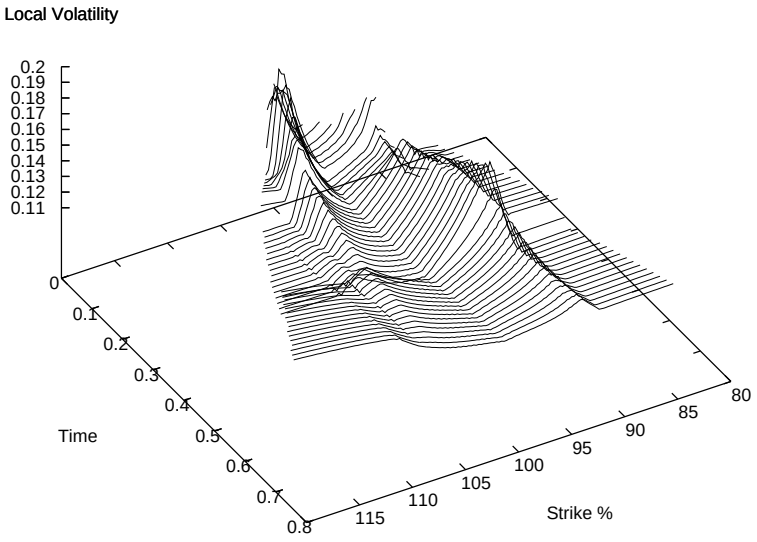

Figure 5: Local volatilities on the USD/DEM exchange rate on August 1995 in terms of the time and spot.

Derman, E. and Kani, I. 1994. Riding on a smile, *Risk* **7**(2): 32–39.

Rubinstein, M. 1994. Implied binomial trees, *Journal of Finance* **49**: 771–818.

Rebonato, R. 1999. *Volatility and Correlation*, Wiley.

Kahale, N. 2004. An arbitrage-free interpolation of volatilities, *Risk* **17**(5): 102–106.

Achdou, Y. and Pironneau, O. 2002. Volatility smiles by multilevel least squares, *International Journal of Theoretical and Applied Finance* **5**(6): 619–643.

Dumas, B., Fleming, J. and Whaley, R. 1998. Implied volatility functions: Empirical tests, *Journal Finance* **53**: 2059–2106.

Coleman, T. F., Li, Y. and Verma, A. 1999. Reconstructing the unknown volatility function, *The Journal of Computational Finance* **3**(2): 77–102.

Andersen, L. and Andreasen, J. 2000. Jump diffusion models: volatility smile fitting and numerical methods for pricing, *Review of derivatives research* **4**: 231–262.

Heston, S. 1993. A closed-form solution of options with stochastic volatility with applications to bond and currency options, *The Review of Financial Studies* **16**: 327–343.

Lagnado, R. and Osher, S. 1997. A technique for calibrating derivative security pricing models: numerical solution of an inverse problem, *Journal of Computational Finance* **1**(1): 13–25.

Maturity	Type	Strike	BS price	MC price
30 days	Call	1.5421	0.0070	0.0070
	Call	1.5310	0.0092	0.0093
	Call	1.4872	0.0235	0.0234
	Put	1.4479	0.0092	0.0092
	Put	1.4371	0.0069	0.0070
60 days	Call	1.5621	0.0094	0.0093
	Call	1.5469	0.0127	0.0126
	Call	1.4866	0.0320	0.0323
	Put	1.4312	0.0128	0.0126
	Put	1.4178	0.0099	0.0099
90 days	Call	1.5764	0.0111	0.0112
	Call	1.5580	0.0149	0.0151
	Call	1.4856	0.0379	0.0383
	Put	1.4197	0.0152	0.0153
	Put	1.4038	0.0114	0.0114
180 days	Call	1.6025	0.0142	0.0144
	Call	1.5779	0.0190	0.0194
	Call	1.4823	0.0505	0.0510
	Put	1.3902	0.0217	0.0218
	Put	1.3682	0.0163	0.0164
270 days	Call	1.6297	0.0173	0.0173
	Call	1.5988	0.0227	0.0230
	Call	1.4793	0.0597	0.0599
	Put	1.3710	0.0255	0.0254
	Put	1.3455	0.0191	0.0189

Figure 6: Black-and-Scholes prices and prices obtained via MC simulation on the USD/DEM exchange rate on August 1995.

Li, Y. 2001. A new algorithm for constructing implied binomial trees: does the implied model fit any volatility smile?, *Journal of Computational Finance* **4**(2): 69–95.

Avellaneda, M., Friedman, C., Holmes, R. and Samperi, D. 1997. Calibrating volatility surfaces via relative-entropy minimization, *Applied Mathematical Finance* **4**(1): 37–64.

Crépey, S. 2003a. Calibration of the local volatility in a generalized black–scholes model using Tikhonov regularization, *SIAM Journal on Mathematical Analysis* **34**(5): 1183–1206.

Crépey, S. 2003b. Calibration of the local volatility in a trinomial tree using Tikhonov regularization, *Inverse Problems* **19**: 91–127.

Press, W. H., Flannery, B. P., Teukolsky, S. A. and Vetterling, W. T. 1993. *Numerical Recipes in C : The Art of Scientific Computing*, Cambridge University Press.

Overhaus, M., Ferraris, A., Knudsen, T., Milward, R., Nguyen-Ngoc, L. and Schindlmayr, G. 2002. *Equity Derivatives, Theory and Applications*, Wiley, John & Sons, Incorporated.